Chemical Engineering Journal 112 (2005) 57–72

Chemical Engineering Journal

www.elsevier.com/locate/cej

Optimization of reactive simulated moving bed and Varicol systems for hydrolysis of methyl acetate

Weifang Yu, K. Hidajat, Ajay K. Ray *

Department of Chemical and Biomolecular Engineering, National University of Singapore, 10 Kent Ridge Crescent, Singapore 119260, Singapore

Received 25 February 2005; received in revised form 24 June 2005; accepted 29 June 2005

Abstract

In this article, multi-objective optimization technique was applied to improve the performance of simulated moving bed reactor (SMBR) and its modification, Varicol process for hydrolysis of methyl acetate. The optimization problems of interest considered are simultaneous maximization of purity and yield of acetic acid and methanol, respectively, in the raffinate and extract streams. The effect of distributed feed flow rate on the performance of SMBR and the applicability of reactive Varicol systems were also investigated. The non-dominated sorting genetic algorithm (NSGA) was used in obtaining Pareto optimal solutions. It was observed that reactive Varicol performs better than SMBR due to non-synchronous switching and its increased flexibility in distributing columns in various sections.

Keywords: Moving bed reactor; Multi-objective optimization; SMBR; Varicol; Methyl acetate; Hydrolysis; Genetic algorithm; Pareto; Multifunctional reactor

1. Introduction

In order to obtain more valuable compound, large amount of by-product, methyl acetate (MeOAc), is usually hydrolysed to methanol (MeOH) and acetic acid (HOAc) in industrial polyvinyl alcohol plant, which are recycled to the methanolysis reaction of polyvinyl acetate and the synthesis of vinyl acetate, respectively. However, the conversion of MeOAc is low in the traditional process consisting of a packed bed reactor followed by a series of distillation columns for the separation of components, due to the equilibrium limitation [1,2].

Combination of chemical reaction and separation in a single apparatus could enhance the conversions of thermodynamic equilibrium-limited reactions and simultaneously obtain high purity products. This is achieved by separating products when they are formed, which in turn shifts the equilibrium toward the desired products. The simulated countercurrent moving bed reactor (SMBR) (see Fig. 1a) is such an integrated reactor-separator that could be employed to enhance the conversion of hydrolysis of MeOAc, leading to less energy cost and higher efficiency of the process. Quite a few studies [3–13] have shown that substantial improvements in the process performance could be achieved in SMBR and in recent years promised its application in fine chemical and pharmaceutical industry. More recently, SMB was modified into Varicol process [14] (see Fig. 1b) by introducing non-synchronous shifting of the inlet and outlet ports during a global switching period. This endowed more flexibility in terms of varied column configuration at different sub-time intervals compared to traditional more rigid SMB process.

The optimal design and selection of optimal operating parameters are essential to realize economic potential of SMBR and Varicol process and its successfully implementation on industrial scale. Although several studies [15–17] have been reported on the optimization of SMBR and Varicol, they only involved single objective optimization in terms of maximization of productivity, which is usually not sufficient for the real-life design of complex SMBR systems, since the operating variables influence the productivity and other important objectives, such as product purity, eluent consumption, etc. usually in conflicting ways. This leads to unfavorable change in the second objective function whenever a

* Corresponding author. Present address: Department of Chemical and Biochemical Engineering, University of Western Ontario, London, Ont., Canada N6A 5B9. Tel.: +1 519 661 2111; fax: +1 519 661 3498.
E-mail address: aray@eng.uwo.ca (A.K. Ray).

1385-8947/$ – see front matter © 2005 Elsevier B.V. All rights reserved.
doi:10.1016/j.cej.2005.06.008

Nomenclature

C	liquid phase concentration (mol/l)
D	apparent axial dispersion coefficient (m^2/s)
k	reaction rate constant
K	equilibrium constant
L	length of column (m)
N	number of switching, column
p	number of columns in section P
P	purity, section P
q	solid phase concentration, number of columns in section Q
Q	volume flow rate (cm^3/min), section Q
r	number of columns in section R
R	reaction rate, section R
s	number of columns in section S
S	selectivity, section S
t	time (min)
T	temperature (K)
u	superficial velocity (m/s)
X	conversion
Y	yield
z	axial coordinate (cm)

Greek letters

α	fraction of feed
β	fraction of raffinate
γ	fraction of desorbent
ε	void fraction
ϕ	section

Subscripts/superscripts

o	initial, inlet
col	column
e	equilibrium
E	extract
f	feed, forward
i	component i
j	column number
g	gas, carrier
HOAc	acetic acid
MeOAc	methyl acetate
MeOH	methanol
N	number, switching period
P	section P
Q	section Q
R	section R
S	switching, section S, solid

desirable change in the first objective function is achieved. Therefore, the simultaneous optimization of multiple objective functions is very important for the design of SMB and Varicol process.

The principle of multi-criterion optimization with conflicting objectives is different from that of single objective optimization [18,19]. Instead of trying to find the best (global) design solution, the goal of multi-objective optimization is to obtain a set of equally good (non-dominating) solutions, which are known as Pareto optimal solutions. In a set of Pareto solutions, no solution can be considered better than any other solutions with respect to all objective functions. The choice of a solution over the other solutions requires additional knowledge of the problem, and often this knowledge is intuitive and non-quantifiable. However, by narrowing down the choices, the Pareto set does provide decision makers with useful guidance in selecting the desired operating conditions (called the preferred solution) from among the (restricted) set of Pareto optimal solutions, rather than from a much larger number of possibilities.

In this article, a comprehensive multi-objective optimization study of SMBR and Varicol processes is reported. The non-dominated sorting genetic algorithm (NSGA) [20] was applied in obtaining Pareto optimal solutions. The multi-objective optimization problems were formulated aiming at are simultaneous maximization of (a) purity and (b) yield of acetic acid and methanol, respectively, in the raffinate and extract streams. The effect of distributed feed flow rate on the performance of SMBR and the applicability of reactive Varicol systems were also investigated. By performing multi-objective optimizations, we are able to deepen the understanding of the SMBR and Varicol processes and meanwhile generate a wider range of alternative optimal operating conditions as the guidance for decision makers.

1.1. Mathematical model

Fig. 1a shows a schematic diagram of a 6-column SMB and the principle of its operation. It consists of columns of uniform cross-section, each of length L and packed with an adsorbent. The columns are connected in series in a circular array. Two incoming fluid streams (feed, F and eluent, E) and two outgoing fluid streams (raffinate, Ra and extract, Ex) divide the system into four sections, with 2, 1, 1 and 2 columns in each section, respectively, corresponding to the column configuration 2/1/1/2. The flow rate in section P (feed section), Q_P, was chosen as the reference flow rate based on which all other flow rates were described. The ratios of the feed flow rate, F, the raffinate flow rate, Ra, the eluent flow rate, E, to that in section P (Q_P) were designated as α, β, γ, respectively. By advancing the introduction and withdrawal ports simultaneously, column by column, in the direction of fluid flow at a predetermined time interval (switching time, t_s), the simulation of countercurrent movement of the solid phase toward the fluid phase is achieved. In SMBR, switching time and column configuration (the number of columns in each section) are decided a priori and is kept constant throughout the entire operation.

In contrast to SMB, Varicol process is based on non-simultaneous and unequal shift of the inlet/outlet ports. The

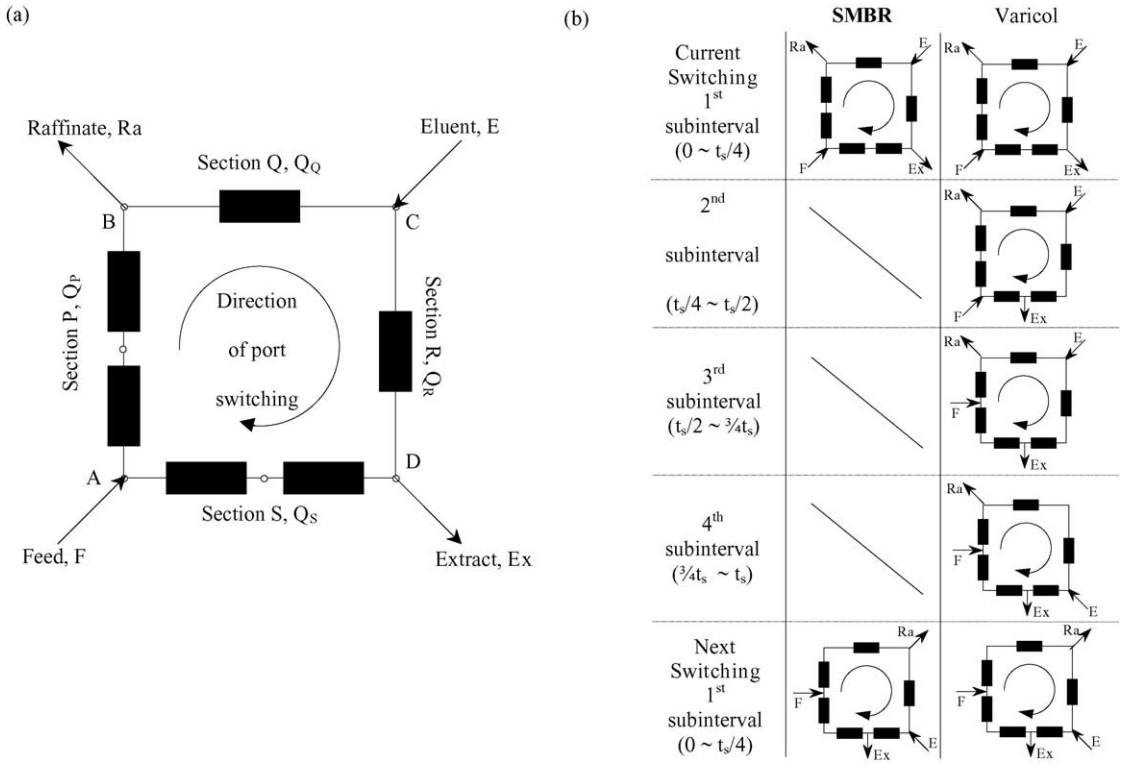

Fig. 1. (a) Schematic diagram of a 6-column SMBR system. (b) Principle of operation of SMBR and 4-sub-interval Varicol (port switching schedule). The inlets and outlets divide the entire system into four sections: P, Q, R, and S with, respectively, 2, 1, 1 and 2 number of columns. The flow rates in each section is given by $Q_Q = (1-\beta)\,Q_P$, $Q_R = (1-\beta+\gamma)\,Q_P$ and $Q_S = (1-\alpha)\,Q_P$, where α, β, γ are given by F/Q_P, Ra/Q_P, E/Q_P.

concept and the principle of operation of the Varicol process is illustrated schematically in Fig. 1b for one switching period. The switching time t_s, which is related directly to the solid flow rate in SMB, is also a key parameter in the Varicol process, although the relationship is not straightforward. In Varicol operation, a non-synchronous shift of the inlet and outlet ports is usually employed within a switching period, which is again kept constant in time. This is shown as an illustrative example in Fig. 1b for a 4-sub-interval Varicol process. Within one (global) switching period t_s, the column configuration changes from 2/1/1/2 (0–t_s/4) to 2/1/2/1 (t_s/4–t_s/2) by shifting the extract port by one column forward, then to 1/1/2/2 (t_s/2–t_s3/4) by shifting the feed port one column forward, then to 1/2/1/2 (t_s3/4–t_s) by shifting the eluent port one column forward, and finally returns back to the original configuration of 2/1/1/2 by shifting the raffinate port one column forward. As a result, in a 4-sub-interval Varicol process, there are four different column configurations for the four sub-intervals due to local switching during one global switching period. The number of columns in each zone varies with time within a global switching period, but the number of columns in each zone returns to the starting value at the end of the global switching period. In terms of average number of columns per zone this corresponds to the configuration 1.5/1.25/1.5/1.75. Note that the average number for any particular zone is obtained as follows: For example, for zone P, 1.5 is obtained from (2 + 2 + 1 + 1)/4, where the numbers in the bracket is the number of columns in zone P in the 4-sub-intervals. Therefore, locations of input/output ports in Varicol processes are quite different from SMB processes. Note that in principle it is possible that a port may shift more than once during one global switching period, either forward or even in backward direction. As a result, Varicol processes can have several column configurations, which endow more flexibility compared to SMB processes. SMB processes can be regarded as a special case of the more flexible Varicol processes. It is remarkable that the Varicol process does not add any additional fixed cost.

In hydrolysis of methyl acetate in SMBR, water is present in large excess concentration. The polymer (Amberlyst 15) resin is initially saturated with water, and therefore, it is assumed that the ion exchange resin in contact with polar solvent (water) is completely swollen, the active sulfonic acid group is totally dissociated, and the solvated protons are evenly distributed in the polymer phase. This enables the chemical species participating in the reaction to penetrate the network of cross-linked polymer chains easily, and come in contact with the solvated protons. Therefore, the quasi-homogeneous model [21] can be applied to describe the reaction. However, when the concentration of water decreases, the polymer phase deviates much from the ideal homogenous state, an absorption-based heterogeneous model would be more suitable. As the reaction is carried out in a large excess of water in this study, the concentration of water can

Table 1
Adsorption constant, K_i, kinetic parameters, k_f, K and dispersion coefficients, D_i [22]

T (K)	K_{MeOH}	K_{HOAc}	$K_{MeOAc} \times 10^1$	$D_{MeOH} \times 10^6$ (m^2/s)	$D_{HOAc} \times 10^6$ (m^2/s)	$k_f \times 10^2$ (s^{-1})	K_e (mol/l)	X_e (%)	Y_e (%)	P_e (%)
313	1.02	0.74	7.05	6.30	7.09	1.25	8.89	90.25	90.25	47.44
318	0.96	0.72	6.90	6.49	6.11	1.87	9.36	91.25	91.15	47.69
323	0.93	0.65	6.86	6.30	6.07	2.57	9.54	92.16	92.16	47.96

Calculation is based on $[MeOAc]_o = 1.0$ mol/l; $X_e = 1 - [MeOAc]_{out}/[MeOAc]_o$; $Y_E = [HOAc]_{out}/[MeOAc]_o$; $P_E = [HOAc]_{out}/([MeOAc]_{out} + [HOAc]_{out} + [MeOH]_{out})$.

be assumed to remain essentially unchanged in the course of the reaction. Based on the above assumptions, the quasi-homogeneous kinetic model, applicable to this work can be written as:

$$R = k_f \left[q_{MeOAc} - \frac{q_{HOAc} q_{MeOH}}{K_e} \right] \tag{1}$$

where R denotes the reaction rate, q_i the concentration of component i (MeOAc, MeOH, or HOAc) in the solid phase, k_f the forward reaction rate constant and K_e represents the reaction equilibrium constant. The concentration of adsorbed species i in the solid phase is computed by assuming that the local liquid and solid phases are in equilibrium and linear adsorption isotherm is applicable. So, it is expressed as:

$$q_i = K_i C_i \tag{2}$$

where K_i and C_i are the adsorption equilibrium constant and liquid phase concentration of component i, respectively. It should be noted that the linear isotherm is only valid when the concentration of the adsorbed components are dilute in the bulk liquid phase, as is the case in this study. When the concentrations of the reactants and products are not sufficiently low, non-linear adsorption models, such as Langmuir model, should be considered in order to describe adsorption process accurately.

Based on the proposed reaction kinetics and adsorption isotherms, the dynamic model for a fixed-bed chromatographic reactor corresponding to each single column in the SMBR unit was developed by adopting equilibrium-dispersive model. Mass balance equations for each component i are written as follows:

$$\frac{\partial C_i}{\partial t} + \left(\frac{1-\varepsilon}{\varepsilon}\right)\frac{\partial q_i}{\partial t} + \frac{u}{\varepsilon}\frac{\partial C_i}{\partial z} - \left(\frac{1-\varepsilon}{\varepsilon}\right)\nu_i R = D_i \frac{\partial^2 C_i}{\partial z^2} \tag{3}$$

The initial and boundary conditions are:

$$C_i[t=0] = C_i^0 \tag{4a}$$

$$C_i(0 < t < t_p)_{z=0} = C_{f,i} \tag{4b}$$

$$C_i(t > t_p)_{z=0} = 0 \tag{4c}$$

$$\left[\frac{\partial C_i(t)}{\partial z}\right]_{z=0} = 0 \tag{4d}$$

The kinetic, adsorption constants and diffusion coefficients of each component involved in the process are listed in Table 1. They were determined semi-empirically by fitting the experimentally measured breakthrough curves with model prediction obtained by solving the above mass balance equations. Detailed procedure is described elsewhere [22].

SMBR unit resembles fixed-bed chromatographic reactor except at the instant of column rotating, and therefore, the dynamic behavior of the SMBR unit can be described by the mathematical model of a single reactive chromatographic column while incorporating the cyclic port switching. The modified mass equations are given by:

$$\frac{\partial C_{ij}^{(N)}}{\partial t} + \left(\frac{1-\varepsilon}{\varepsilon}\right)\frac{\partial q_{ij}^{(N)}}{\partial t} + \frac{u_\phi}{\varepsilon}\frac{\partial C_{ij}^{(N)}}{\partial z} - \left(\frac{1-\varepsilon}{\varepsilon}\right)\nu_i R_j^{(N)} = D_i \frac{\partial^2 C_{ij}^{(N)}}{\partial z^2} \tag{5}$$

for the component i in the jth column during the Nth switching period, u_ϕ denotes superficial flow rate in section ϕ (where ϕ = P, Q, R, S), and the reaction rate expression and adsorption isotherms are given by:

$$R_j^{(N)} = k_f \left[q_{MeOAc,j}^{(N)} - \frac{q_{HOAc,j}^{(N)} q_{MeOH,j}^{(N)}}{K_e} \right] \tag{6}$$

$$q_{ij}^{(N)} = K_i C_{ij}^{(N)} \tag{7}$$

The initial and boundary conditions are:

Initial condition:

$$\text{When } N = 0,\ C_{ij}^{(0)} = C_{ij}^{\text{Initial}} = 0 \tag{8a}$$

When $N \geq 1$,

$$C_{ij}^{(N)} = C_{i,j+1}^{(N-1)} \quad \text{for} \quad j = 1 \sim (N_{col} - 1) \tag{8b}$$

$$C_{ij}^{(N)} = C_{i1}^{(N-1)} \quad \text{for} \quad j = N_{col} \tag{8c}$$

Boundary conditions:Feed entry point (point A in Fig. 1)

$$C_{i1}^{(N)}|_{z=0} = (1-\alpha) C_{i,N_{col}}^{(N)}|_{z=L} + \alpha C_{i,f} \tag{9a}$$

Raffinate take-off point (point B in Fig. 1)

$$C_{i,p+1}^{(N)}|_{z=0} = C_{i,p}^{(N)}|_{z=L} \tag{9b}$$

Eluent inlet point (point C in Fig. 1)

$$C^{(N)}_{i,p+q+1}|_{z=0} = \left[\frac{1-\beta}{1-\beta+\gamma}\right] C^{(N)}_{i,p+q}|_{z=L} \tag{9c}$$

Extract take-off point (point D in Fig. 1)

$$C^{(N)}_{i,p+q+r+1}|_{z=0} = C^{(N)}_{i,p+q+r}|_{z=L} \tag{9d}$$

The mass balance Eq. (5), initial Eq. (8) and boundary conditions Eq. (9), kinetic equation Eq. (6) and adsorption isotherm Eq. (7) completely define the SMBR system. The PDEs were solved using Method of Lines. The PDEs were first discretized in space using Finite Difference Method (FDM) to convert it into a set of several-coupled ODE–IVPs and the resultant stiff ODEs of the initial value kind were solved using the subroutine, DIVPAG, in the IMSL library. Since periodic switching is imposed on the system, the reactor works under transient conditions. Whenever switching is performed a new initial value problem must be solved. However, a cyclic (periodic) steady-state with a period equal to the switching time is eventually attained. After each switching, column numbering was redefined according to Eq. (10) so that feed is always introduced into the first column.

Before switching	After switching	
Column 1	Column N_{col}	(10)
Column j	Column $j-1$ $\quad j = 2, 3, \ldots, N_{col}$	

The concentration profiles were obtained from the solution of the above equations Eqs. (5)–(10). The dynamic model for Varicol can be easily derived by incorporating the sub-time interval switching into SMBR model. A set of objective functions examined in this work are defined as follows:

2. Sensitivity study

Before formulating optimization problems, a comprehensive parametric sensitivity study was conducted in order to acquire a thorough understanding of the SMBR system. Sensitivity analysis was carried out by changing only one process parameter at a time while fixing the other operating parameters at a reference set of values. Effects of switching time (t_s), flow rates of feed (α), raffinate (β), desorbent (γ), and number of columns (p, q, r and s) in sections P, Q, R and S, respectively, on the several performance criteria, X_{MeOAc}, Y_{MeOH}, Y_{HOAc}, P_{MeOH} and P_{HOAc}, as defined in Eqs. (11)–(15) are shown in Tables 2.1 and 2.2. The parameters on the first row of Tables 2.1 and 2.2 denote x-axis variable for the respective column and the effect of each parameter on X_{MeOAc}, Y_{MeOH}, Y_{HOAc}, P_{MeOH} and P_{HOAc} are shown for reference values of other parameters in the five subsequent rows.

It was found that q and r, which represents numbers of columns in sections Q and R, respectively, have little effect on the performance of the process, when each of them was varied between 1 and 5. Some parameters, such as β and γ, influence the Y_{HOAc}, P_{HOAc}, Y_{MeOH} and P_{MeOH} in conflicting ways. Tables 2.1 and 2.2 reveals that there is a complex interplay of all these parameters on X_{MeOAc}, Y_{MeOH}, Y_{HOAc}, P_{MeOH} and P_{HOAc}. If we want to maximize one, the other one worsens. Optimum SMBR configuration (number and length of columns), and operating conditions (such as t_s, β, γ, etc.) differ depending on which variable we want to maximize among X_{MeOAc}, Y_{MeOH}, Y_{HOAc}, P_{MeOH} and P_{HOAc}, and it may not be possible to maximize all at the same time. Therefore, multi-objective optimization is essential to improve the performance of SMBR.

$$X_{MeOAc} = \frac{(\text{MeOAc fed} - \text{MeOAc collected in raffinate and extract})}{\text{MeOAc fed}} = \frac{\alpha C_{MeOAc,f} t_s - \left[\beta \int_0^{t_s} C^{(N)}_{MeOAc,p}|_{z=L_{col}} dt + (\alpha+\gamma-\beta)\int_0^{t_s} C^{(N)}_{MeOAc,p+q+r}|_{z=L_{col}} dt\right]}{\alpha C_{MeOAc,f} t_s} \tag{11}$$

$$Y_{MeOH} = \frac{\text{MeOH collected in extract}}{\text{MeOAc fed}} = \frac{\beta\left[\int_0^{t_s} C^{(N)}_{MeOH,p+q+r}|_{z=L_{col}} dt\right]}{\alpha C_{MeOAc,f} t_s} \tag{12}$$

$$Y_{HOAc} = \frac{\text{HOAc collected in raffinate}}{\text{MeOAc fed}} = \frac{(\alpha+\gamma-\beta)\left[\int_0^{t_s} C^{(N)}_{HOAc,p}|_{z=L_{col}} dt\right]}{\alpha C_{MeOAc,f} t_s} \tag{13}$$

$$P_{MeOH} = \frac{\text{MeOH collected in extract}}{[\text{MeOH} + \text{MeOAc} + \text{HOAc}]\text{ collected}} = \frac{\int_0^{t_s} C^{(N)}_{MeOH,p+q+r}|_{z=L_{col}} dt}{\int_0^{t_s}(C^{(N)}_{MeOH,p+q+r} + C^{(N)}_{MeOAc,p+q+r} + C^{(N)}_{HOAc,p+q+r})|_{z=L_{col}} dt} \tag{14}$$

$$P_{HOAc} = \frac{\text{HOAc collected in raffinate}}{[\text{MeOH} + \text{MeOAc} + \text{HOAc}]\text{ collected}} = \frac{\int_0^{t_s} C^{(N)}_{HOAc,p}|_{z=L_{col}} dt}{\int_0^{t_s}(C^{(N)}_{MeOH,p} + C^{(N)}_{MeOAc,p} + C^{(N)}_{HOAc,p})|_{z=L_{col}} dt} \tag{15}$$

Table 2.1
Sensitivity of process parameters on the performance of SMB system for the hydrolysis of methyl acetate

	t_s	α	β	γ
Y_{HOAc}	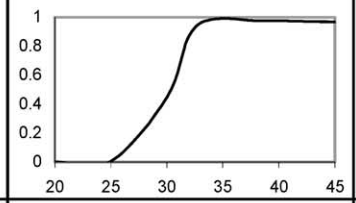	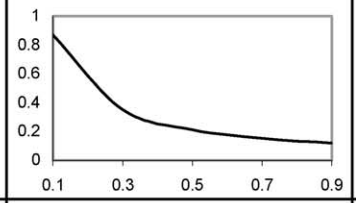	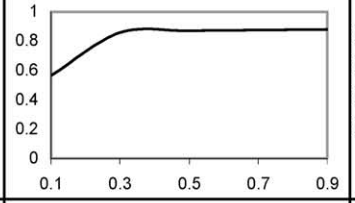	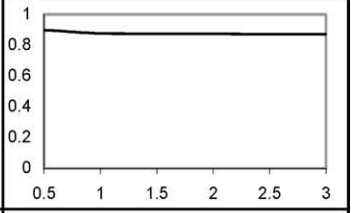
P_{HOAc}	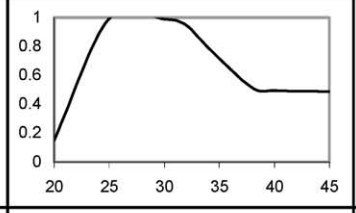	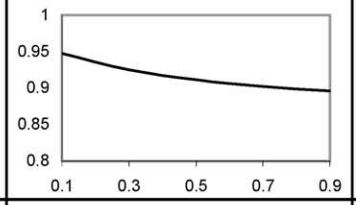	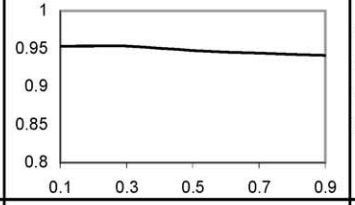	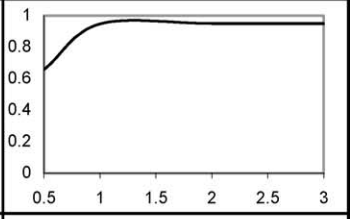
X_{MeOAc}	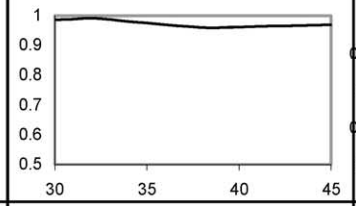	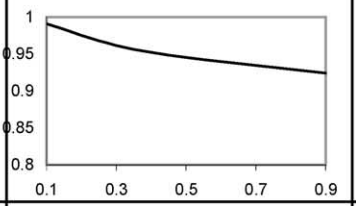	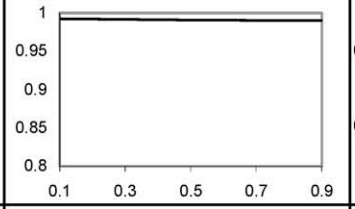	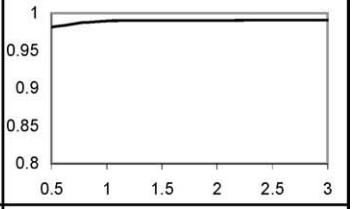
Y_{MeOH}	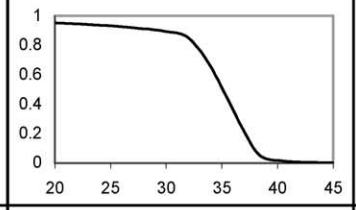	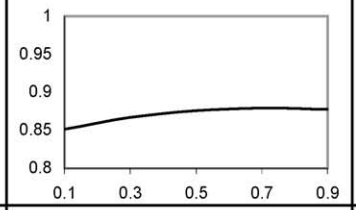	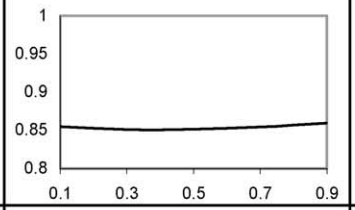	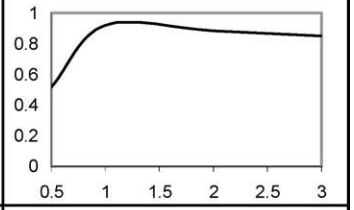
P_{MeOH}	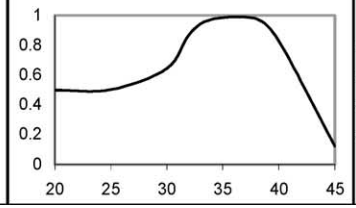	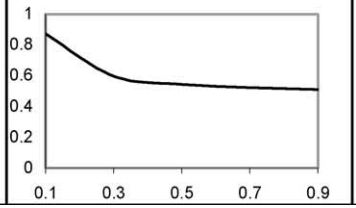	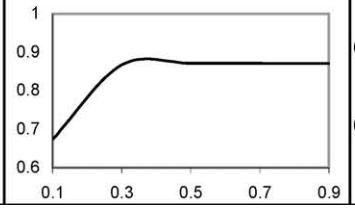	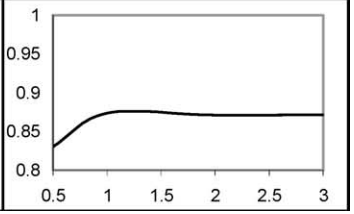

Reference values: $Q_P = 1$ ml/min; $L = 25$ cm; $\varepsilon = 0.4$; $C_{HOAC,\,f} = 1$ mol/l; $\alpha = 0.1$, $\beta = 0.5$, $\gamma = 3.0$, $p = s = 2$, $q = r = 1$.

Table 2.2
Sensitivity of process parameters on the performance of SMB system for the hydrolysis of methyl acetate

	p	q	r	s
Y_{HOAc}	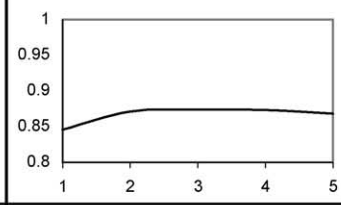	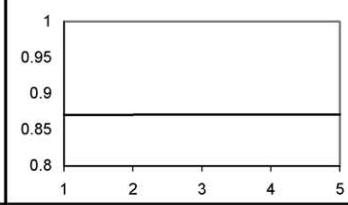	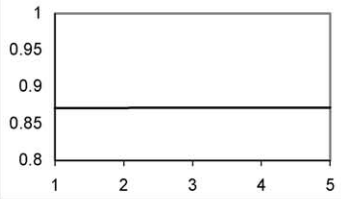	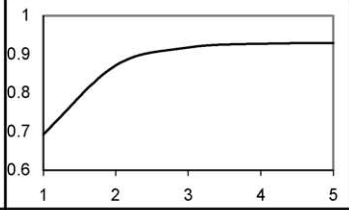
P_{HOAc}	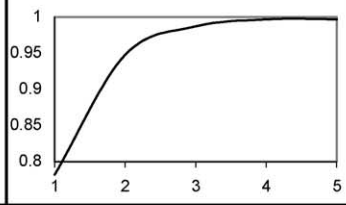	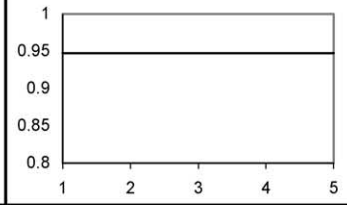	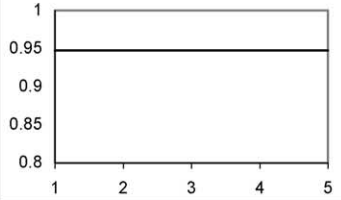	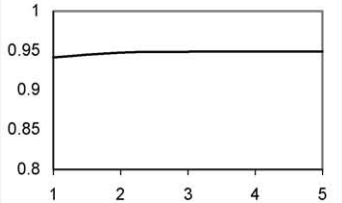
X_{MeOAc}	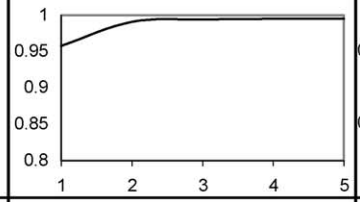	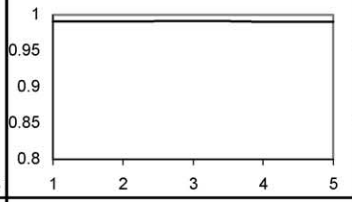	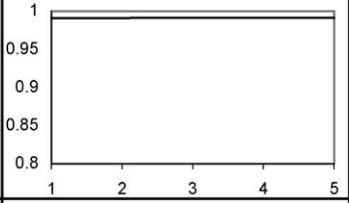	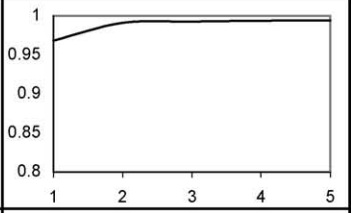
Y_{MeOH}	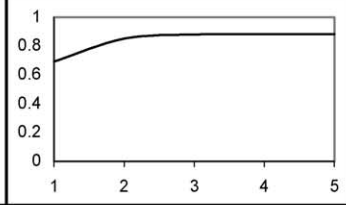	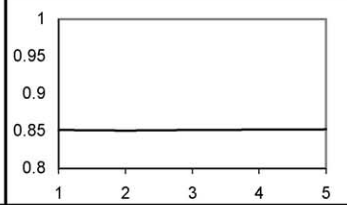	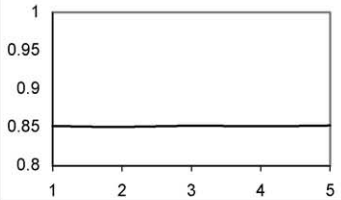	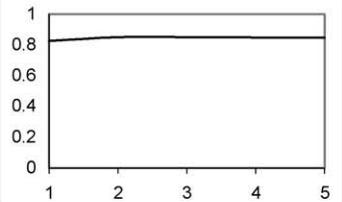
P_{MeOH}	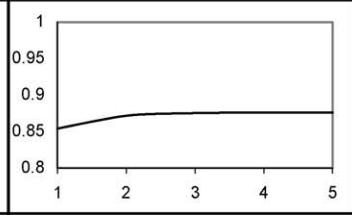	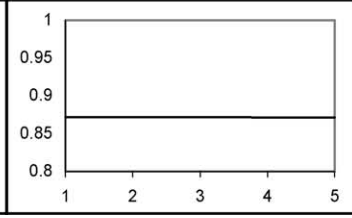	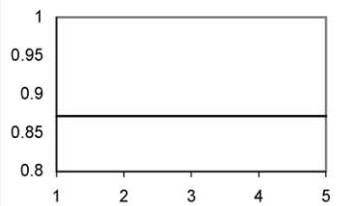	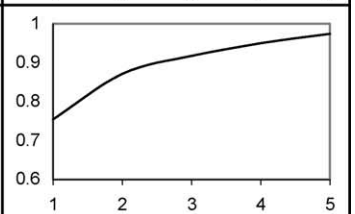

Reference values: $Q_P = 1$ ml/min; $L = 25$ cm; $\varepsilon = 0.4$; $C_{HOAC,\,f} = 1$ mol/l; $\alpha = 0.1$, $\beta = 0.5$, $\gamma = 3.0$, $p = s = 2$, $q = r = 1$.

3. Optimization of SMBR and Varicol systems

3.1. Case 1: maximization of purity of both raffinate and extract streams

In industrial polyvinyl alcohol plant, both of the products (MeOH and HOAc) from the hydrolysis of MeOAc are desirable, since they can be recycled to the methanolysis reaction of polyvinyl acetate and the synthesis of vinyl acetate, respectively. Therefore, it is meaningful to formulate the optimization problem aiming at simultaneous maximization of purity of acetic acid (P_{HOAc}) in raffinate stream and purity of methanol (P_{MeOH}) in extract stream. In addition, since the cost of the adsorbent is always one of the key factors in evaluating the economic potential of SMBR plants, the performance of SMBR was, therefore, optimized at the design stage to determine the optimal length of columns for a 7-column SMBR unit. The optimization problem is described in Table 3.

The optimal solutions with respect to maximization of purity of both raffinate and extract streams and corresponding decision variables are shown in Fig. 2. From Fig. 2a, it can be observed that P_{HOAc} in raffinate stream increases at the cost of decreasing P_{MeOH} in extract stream, which is in agreement with the result obtained from the sensitivity study. The figure also shows that raffinate flow rate (β) and eluent flow rate (γ) are scattered, implying that they are relatively insensitive in deciding the Pareto solutions, as long as they are sufficiently large for the retention of HOAc in section Q and regeneration of adsorbent in section R, respectively. This is validated later by investigating the effects of raffinate and eluent flow rates on the shift of Pareto solutions. The switching time slightly increases as P_{MeOH} in the extract stream increases, and it is also evident from the figure that more columns are needed in section S in order to improve P_{MeOH} in the extract stream. Fig. 3 compares the cyclic steady-state concentration profiles for two points (shown as 1 and 2 in Fig. 2) in the Pareto set. It is evident from the figure that the concentration fronts of HOAc and MeOH in section S are better separated when more columns are present in section S with slightly greater switching time, leading to higher P_{MeOH} in the extract stream. The optimal number of columns in sections Q and R are both equal to 1, which is expected since sections P and S are the key sections for complete conversion and separation while sections Q and R are mainly responsible for regeneration of solvent and adsorbent, respectively. The optimal length of column was found to be about 0.87 m.

3.2. Case 1a: effect of the column length, L_{col}

The effect of column length on the Pareto optimal solutions was studied in order to find a suitable column length, since the obtained optimal length of column for a 7-column SMBR unit was too long compared with the diameter of the column. Thus, the optimization problem was formulated by fixing the length of column as 20, 30 and 50 cm. The formulation of the optimization problem is given in Table 3. Fig. 4 shows that the performance of a 7-column SMBR unit is satisfying when each of the columns is 30 cm long, as both of the purity of raffinate and extract streams can reach 90%. Therefore, in all the following cases, the column length is fixed as 30 cm.

3.3. Case 1b: effect of raffinate flow rate, β

In Case 1, it was observed that raffinate flow rate was relatively insensitive in deciding the optimal solutions. In this section, the Pareto solutions were determined for three different raffinate flow rates. The optimization formulation is provided in Table 3. It is shown by Fig. 5 that there was no significant shift of Pareto's when the raffinate flow rate was reduced from 0.8 to 0.4. This is in agreement with the results obtained in Case 1.

Table 3
Description of the multi-objective optimization problems solved together constraints, bounds of decision variables, and fixed parameters

Case	Objective	Constraint	Decision variables	Fixed parameters
1	Max P_{HOAc}, Max P_{MeOH}	$X_{MeOAc} \geq 90\%$, $P_{HOAc} \geq 80\%$, $P_{MeOH} \geq 80\%$	$30 \leq t_s \leq 60$ min, $3 \leq \gamma \leq 5$, $0.1 \leq \beta \leq 0.9$, $20 \leq L \leq 100$ cm, $1 \leq s \leq 3$, $1 \leq q, r \leq 2$	$d_{col} = 0.94$ cm, $N_{col} = 7$, $Q_P = 1$ ml/min, $\alpha = 0.1$, C^{feed}_{HOAc}=1 mol/l, $T = 318$ K
1a			$10 \leq t_s \leq 60$ min, $3 \leq \gamma \leq 5$, $0.1 \leq \beta \leq 0.9$, $1 \leq s \leq 3$	Same as Case 1 except $L = 20$, 30, 50 cm, $q = 1$, $r = 1$
1b			$10 \leq t_s \leq 30$ min, $3 \leq \gamma \leq 5$	Same as Case 1 except $L = 30$ cm, $\beta = 0.4$, 0.6, 0.8, $p = 2$, $q = r = 1$, $s = 3$
1c			$10 \leq t_s \leq 30$ min	Same as Case 1b except $\beta = 0.8$, $\gamma = 1.0$, 1.5, 2.0, 3.0
1d			$0.0001 \leq \alpha_1, \alpha_2, \alpha_3 \leq 0.3$	Same as Case 1 except[a] $L = 30$ cm, $p = 3$, $q = 1$, $r = 1$, $s = 2$
1e			$10 \leq t_s \leq 30$ min, $3 \leq \gamma \leq 5$, $0.1 \leq \beta \leq 0.9$, $1 \leq s \leq 4$, χ (see Table 5)	Same as Case 1 except $L = 30$ cm, $N_{col} = 6$, 7, 8, $q = 1$, $r = 1$
1f			Same as Case 1e	Same as Case 1e except $N_{sub\text{-}interval} = 3$, 4, 5

[a] Point 1: $\beta = 0.44$, $\gamma = 3.15$, $t_s = 19.5$ min; point 2: $\beta = 0.75$, $\gamma = 4.25$, $t_s = 19.8$ min; point 3: $\beta = 0.69$, $\gamma = 3.40$, $t_s = 19.5$ min.

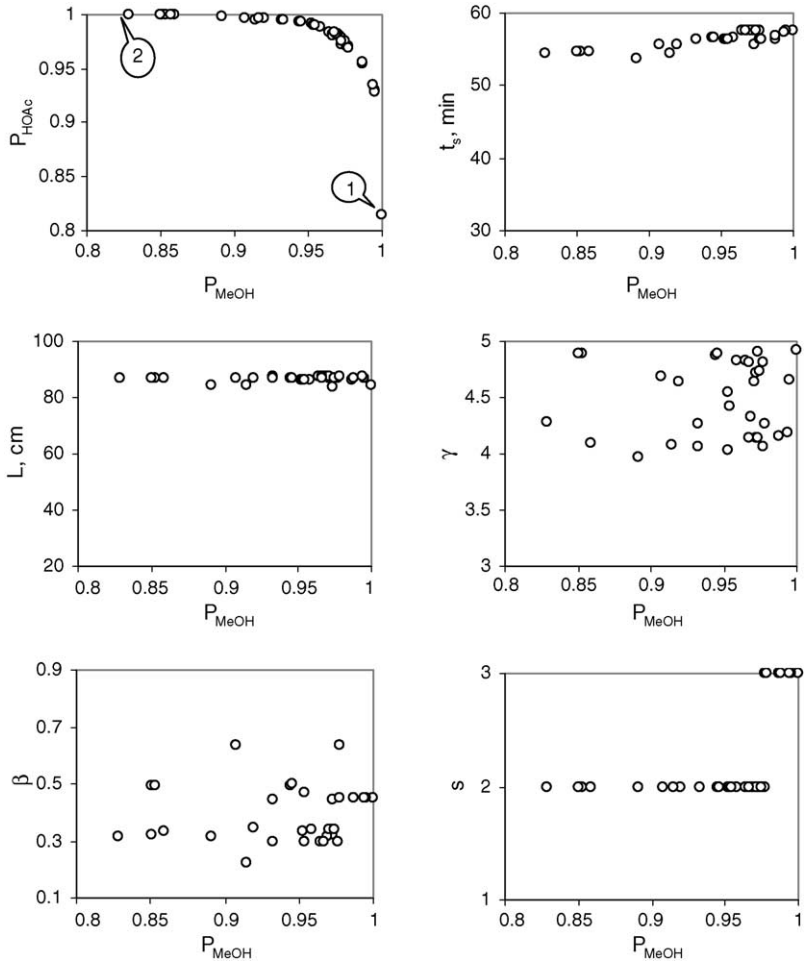

Fig. 2. Pareto optimal solutions and corresponding decision variables for Case 1 optimization problem.

3.4. Case 1c: effect of eluent flow rate, γ

The effect of eluent flow rate on the performance of SMBR was also investigated. The optimization formulation is described in Table 3. Fig. 6 compares the optimal solutions in terms of maximization of purity of both raffinate and extract streams for four different eluent flow rates. When the eluent flow rate was increased from 1.0 to 1.5, a 6.5% improvement in the P_{HOAc} in the raffinate stream was observed for a given P_{MeOH} of about 90%. However, there was no further significant improvement when the eluent flow rate was increased further from 1.5 to 2 or 3. This can be explained by comparing the cyclic steady-state concentration profiles for eluent flow rate as 1.0, 1.5 and 3 as shown in Fig. 7. It was observed that the solid adsorbent is not completely regenerated when the eluent flow rate is 1.0 and the remaining methanol will later contaminate the purity of the raffinate stream. When eluent flow rate is increased to 1.5, the complete regeneration of adsorbent is achieved in section R, leading to improvement in the purity of acetic acid in the raffinate stream.

3.5. Case 1d: effect of distributed feed flow

One of the limitations of the SMB is that during much of the operation, the stationary phase in some of the columns are either completely free of solutes, or contains only product so that the separation capacity is significantly reduced. One way to improve SMB efficiency is to use non-synchronous switching like in Varicol, which is considered later. Alternative option that could improve the effective utilization of adsorbent phase would be to vary the feed flow rate during a global switching interval. Some studies have been reported regarding this mode of operation for non-reactive SMB [23–27]. In order to evaluate the efficacy of this approach, and to determine the extent to which the performance of SMBR could be improved by using variable feed flow rate. The optimization problem for the SMBR with four sub-feed interval is described in Table 3. The operating conditions for the problem solved in this case is identical to the optimum solution obtained corresponding to Case 1a (with $L = 30$ cm) except that the feed flow rate was not kept constant at $\alpha = 0.1$ for the entire switching interval instead allowed to vary according to

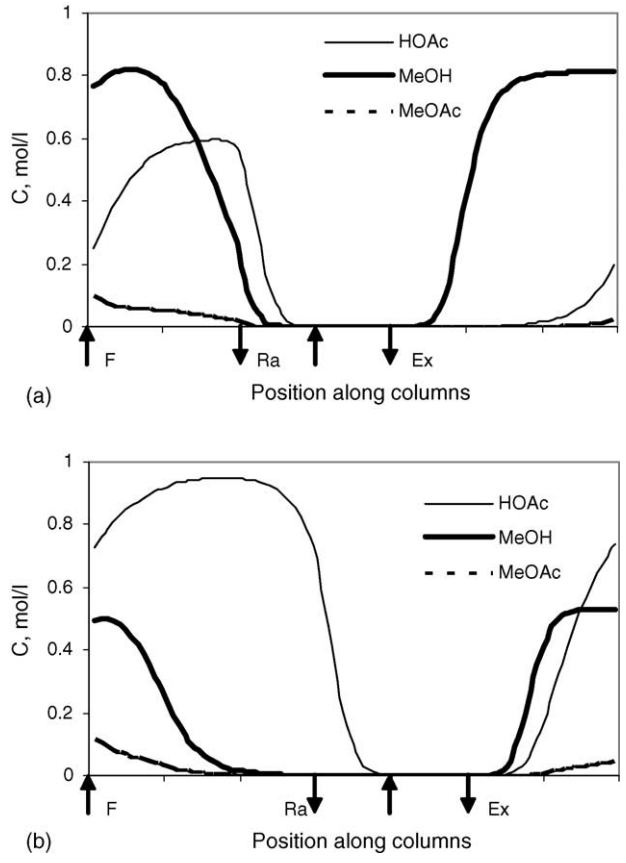

Fig. 3. Concentration profiles of MeOAc–HOAc–MeOH at the end of 100 switching corresponding to (a) point 1 and (b) point 2 in Fig. 2.

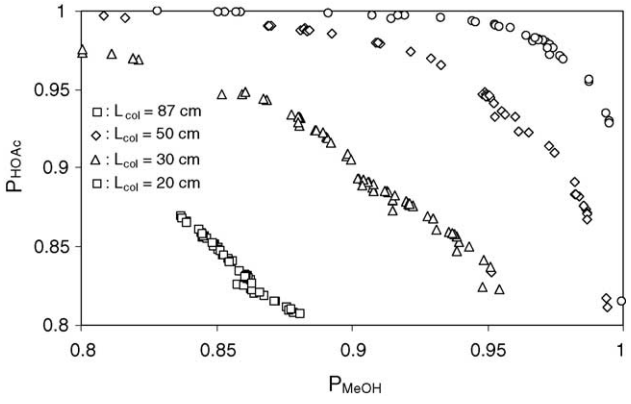

Fig. 4. Comparison of Pareto optimal solutions for different column length (Case 1a).

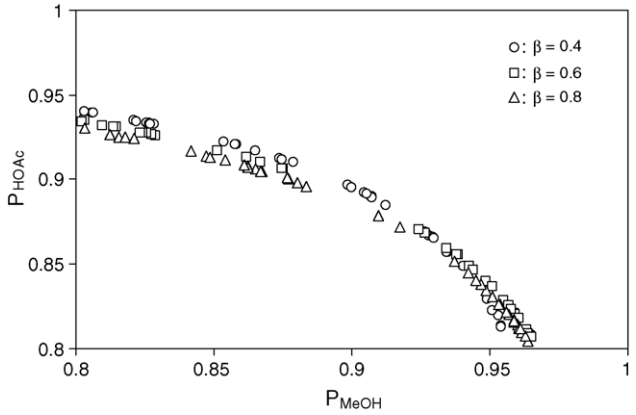

Fig. 5. Effect of raffinate flow rate (β) on the Pareto optimal solutions (Case 1b).

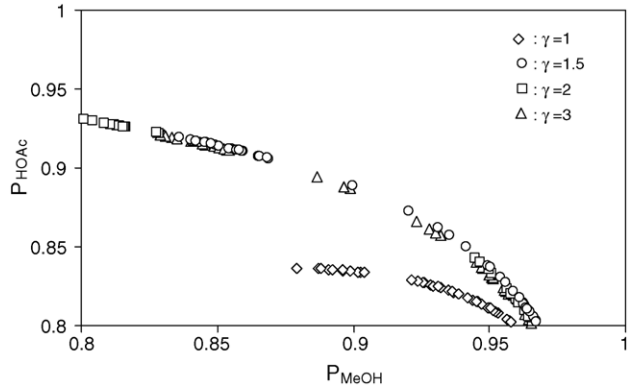

Fig. 6. Effect of eluent flow rate (γ) on the Pareto optimal solutions (Case 1c).

Eq. (16a) while Eq. (16b) is used to ensure that total feed flow rate is same as that of the constant feed flow case (Case 1a in Table 3), and therefore, the optimum results can be compared.

$$1 \times 10^{-4} \leq \alpha_1, \alpha_2, \alpha_3 \leq 0.3 \tag{16a}$$

$$\alpha_4 = 4\alpha - (\alpha_1 + \alpha_2 + \alpha_3) \tag{16b}$$

Fig. 8 shows that by varying the feed flow rate (keeping the total feed flow rate constant), both of the purity of the raffinate and the extract streams can be improved. Table 4 compares the objective function values and the corresponding optimal feed flow rates at the four sub-time intervals for three optimal points with the reference point 2 shown in Fig. 8. It was observed that the distribution of the feed flow rate for all the optimal solutions represents a uniform cyclic (periodic)

Table 4
Comparison of objective function values for constant and variable feed flow rate

Point in Fig. 8	P_{HOAc} (%)	P_{MeOH} (%)	α_1	α_2	α_3	α_4
VF1	91.3	90.2	5.8×10^{-4}	0.132	0.259	7.7×10^{-4}
VF2	91.1	90.5	4.8×10^{-4}	0.174	0.223	3.5×10^{-3}
VF3	91.3	90.2	4.8×10^{-4}	0.128	0.269	2.0×10^{-3}
2	90.7	89.8	$\alpha = 0.1$			

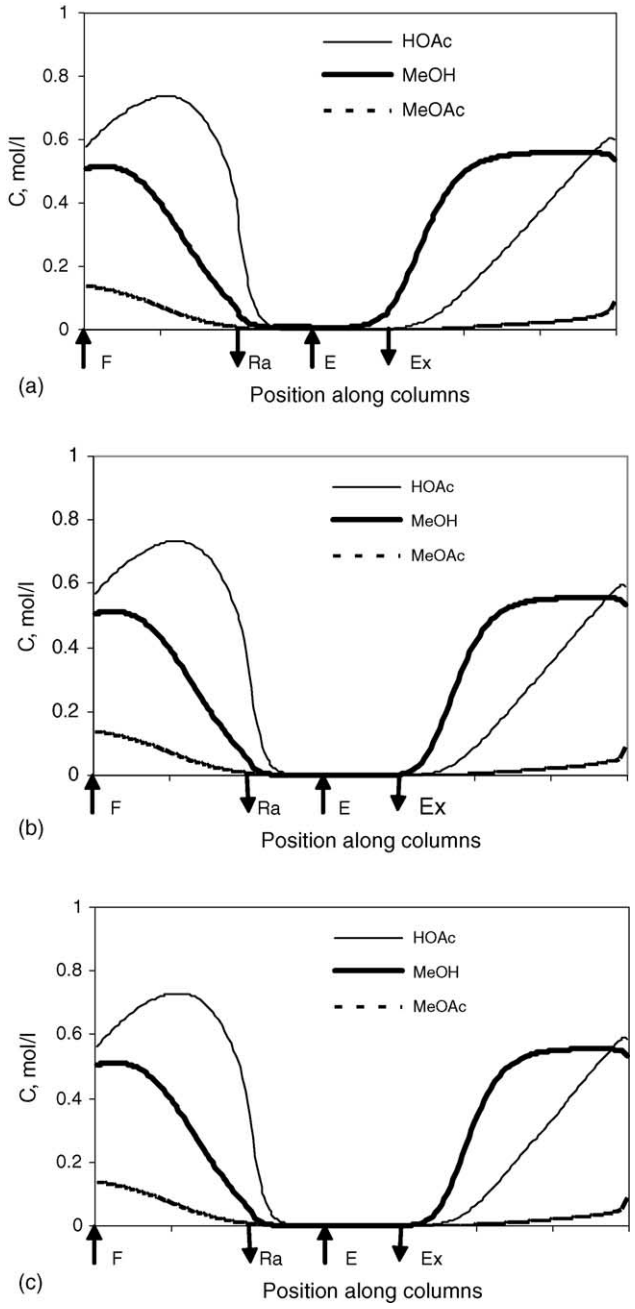

Fig. 7. Concentration profiles of MeOAc–HOAc–MeOH at the end of 100 switching (Case 1c). (a) $\gamma = 1.0$, (b) $\gamma = 1.5$, and (c) $\gamma = 3.0$.

behavior. The feed flow rate (α_1) is extremely small during the first sub-interval, increases to a higher value for the second and the third time interval, and finally decreases to a lower value at the last time interval. The advantage of this particular cyclic behavior for the performance of SMBR can be illustrated by comparing the concentration profiles for constant (point 2) and variable feed flow rate (VF_1) at the end of each of the four sub-time intervals as shown in Fig. 9. The figure shows that the concentration front of MeOH and unreacted MeOAc move faster toward the raffinate port and tends to breakthrough form section P during the last time

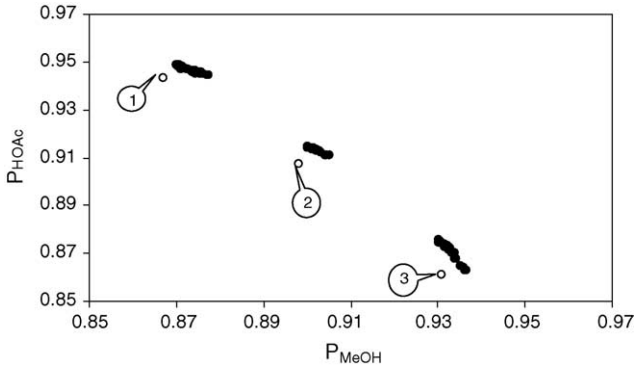

Fig. 8. Comparison of Pareto optimal solutions between constant and distributed feed flow rate (Case 1d).

interval when the feed flow rate is constant. This gives rise to lower purity of HOAc (P_{HOAc}) in the raffinate stream compared to variable feed flow. Likewise, the smaller feed flow rates in the first time interval help to improve the purity of MeOH in extract stream, since HOAc and unreacted MeOAc tend to breakthrough from section S in the first time interval. The forced periodic feed flow rate could improve the performance SMB for other operating conditions also and the extent of improvement vary depending on the specific reaction system, column configuration, and numbers of sub-time intervals employed.

3.6. Case 1e: comparison of the performance of SMBR and Varicol systems

In order to improve the process efficiency, SMB was recently modified into Varicol by introducing the non-synchronous shift of the inlet and outlet ports during a global switching period. It has been reported that Varicol system performs better than its equivalent SMB system due to the flexibility in column distribution [14]. Thus, in this section, the optimization study was carried out to determine to what extent improvement can be obtained for a 4-sub-interval 7-column Varicol system over an equivalent SMBR unit. Furthermore, the performance of 7-column SMBR and Varicol was compared with 6-column Varicol and 8-column SMBR. For 6- and 7-column Varicol, there could exist, respectively, 10 and 20 possible column configurations (χ). Among these configurations, the possible optimal configurations were selected from the simulation studies that lead to better performance of the system and are listed in Table 5. The formulation of the optimization problem is described in Table 3.

The Pareto optimal solutions of the 6- and 7-column Varicol together with 7- and 8-column SMBR and corresponding switching time are illustrated in Fig. 10. Slight improvement in purity for both raffinate and extract streams can be achieved in 7-column Varicol compared to an equivalent SMBR unit. However, 8-column SMBR performs better than 7-column Varicol while the performance of 6-column

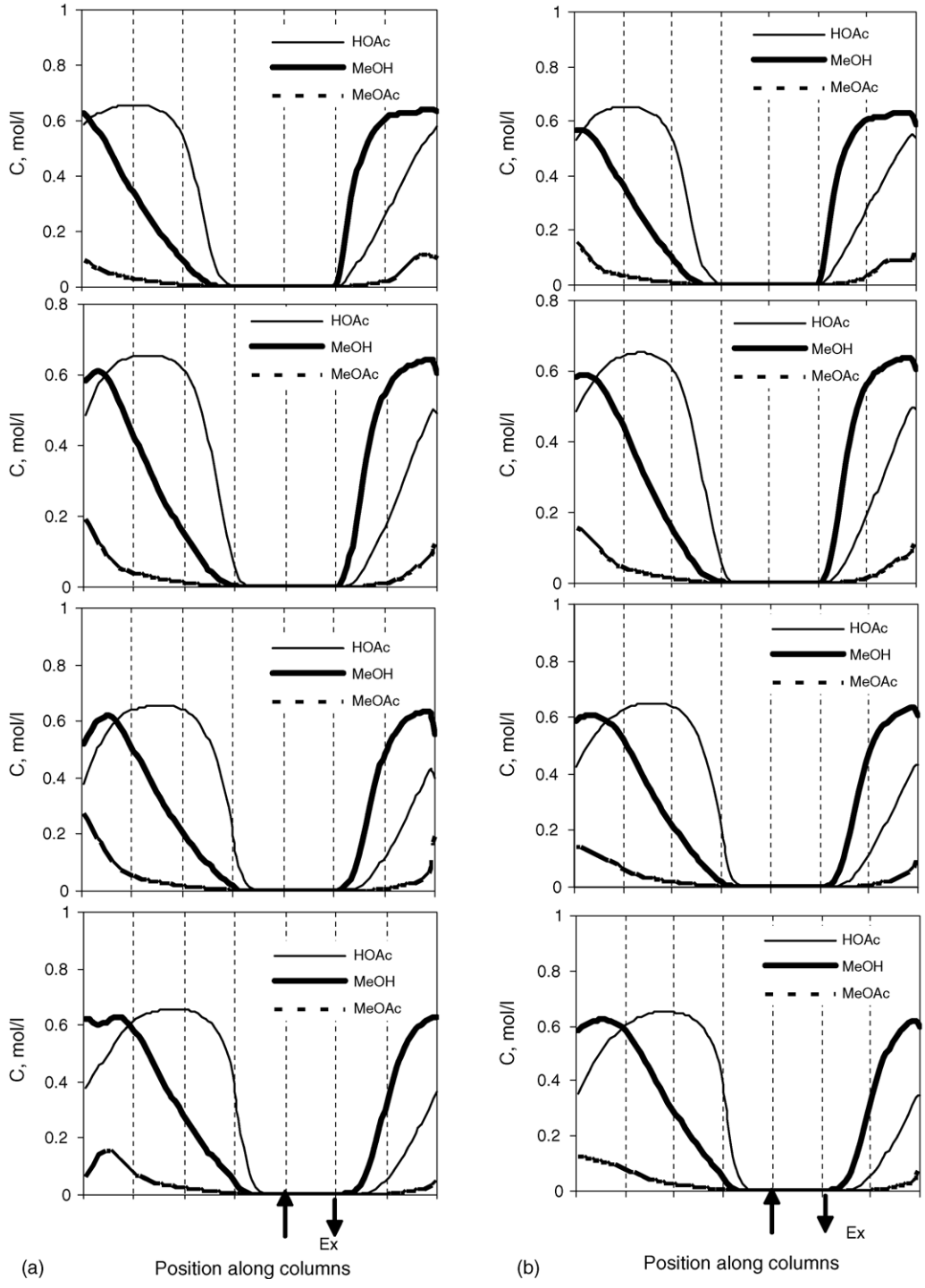

Fig. 9. Concentration profiles for constant and variable feed flow rate the end of sub-time intervals. (a) Variable feed flow rate and (b) Constant feed flow rate (point 2 in Fig. 8).

Varicol is worse than 7-column SMBR. Similar results were reported by Zhang et al. [28] for a non-reactive case that 5-column Varicol performs better than an equivalent SMB unit, while 6-column SMB performs better than 5-column Varicol. The optimal column configurations for the 4-sub-interval 6-column Varicol are C-C-C-A, A-A-C-C and for the 7-column Varicol are B-B-C-C, B-B-B-C, B-C-C-C (see Table 5). The optimal column configurations for 8-column SMBR are 2-1-1-4, 3-1-1-3 and 4-1-1-2. These optimal configurations imply that more columns are needed in sections P or S in order to achieve as high purity for raffinate and extract streams since they are the key sections for complete conversion and separation.

Table 5
List of possible optimal column configurations (χ) for 6- and 7-column Varicol system within a global switching period

χ	Column configuration[a]	χ	Column configuration
$N_{col} = 6$			
A	1/1/1/3	B	2/1/1/2
C	3/1/1/1	D	1/1/2/2
E	2/2/1/1	F	2/1/2/1
G	1/2/1/2	–	–
$N_{col} = 7$			
A	1/1/1/4	B	2/1/1/3
C	3/1/1/2	D	4/1/1/1
E	1/2/1/3	F	1/1/2/3
G	2/2/1/2	H	3/2/1/1
I	2/1/2/2	G	3/1/2/1

[a] Column distribution 3/1/1/1 implies 3 columns in section P and one column each in sections Q to S.

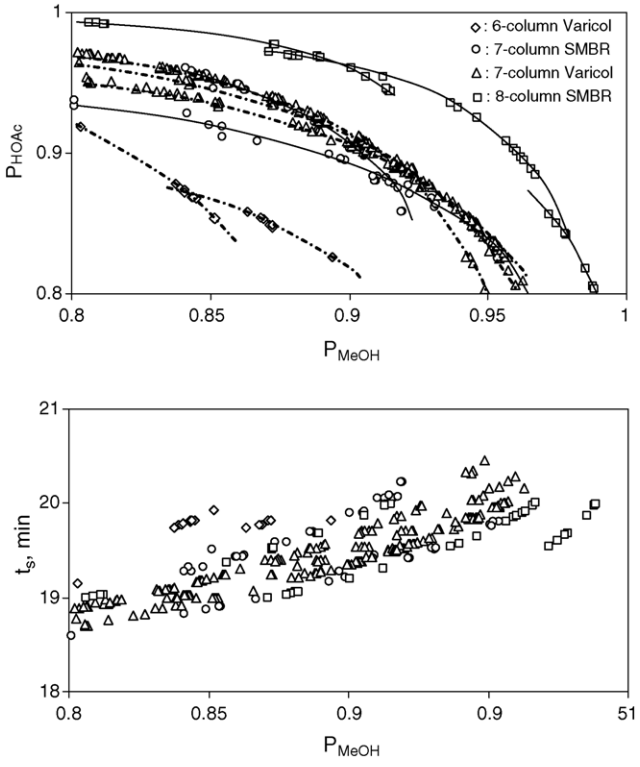

Fig. 10. Comparison of Pareto optimal solutions for 6- and 7-column Varicol together with 7- and 8-column SMB systems (Case 1e).

3.7. Case 1f: effect of number of sub-interval

In Case 1e, 4-sub-interval switching within a global switching period was applied to a 7-column Varicol system.

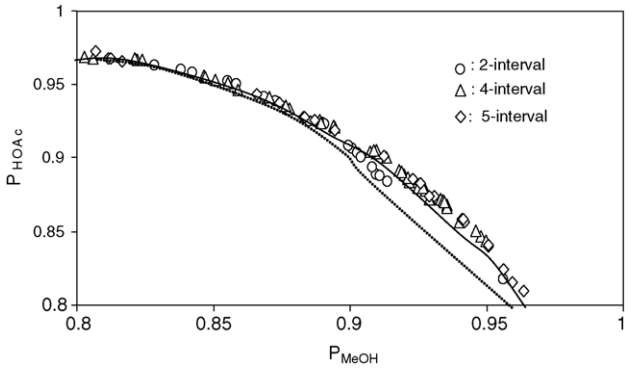

Fig. 11. Effect of number of sub-time interval for 7-column Varicol system (Case 1f).

It is expected that if the number of sub-intervals is increased, better performance could be achieved in Varicol due to additional flexibility in column distribution. Therefore, the effect of number of sub-interval switching on the performance of Varicol was investigated by varying around the reference value of 4 to 3 and 5. Fig. 11 compares the Pareto optimal solutions for the different number of sub-interval switching in 7-column Varicol. When the number of sub-intervals switching was increased from 3 to 4, a 2.3% improvement in the P_{HOAc} was obtained for a given P_{MeOH} of about 91%. However, there was no significant improvement when the number of switching was increased further from 4 to 5, thus 4-sub-interval was found to be sufficient for the effective operation of Varicol system for the hydrolysis of MeOAc. The optimal column configurations (χ) for the 3- and 5-sub-interval are B-C-C, C-C-B or C-C-C and B-C-C-C-C, B-B-C-C-C, B-B-B-C-C or B-B-B-B-C, respectively.

3.8. Case 2: maximization of yield of both raffinate and extract streams

In this case, the optimization problem was formulated in order to obtain as high yield of both the raffinate and extract streams while at the same maintaining the purity of raffinate and extract streams greater that 80%. The mathematically formulation of the problem is described in Table 6. The optimal solutions with respect to maximization of Y_{HOAc} and Y_{MeOH} are illustrated in Fig. 12. The figure demonstrates that one cannot improve yield of acetic acid in the raffinate stream without sacrificing yield of methanol in the extract stream. Moreover, the figure clearly shows that the maximum Y_{HOAc} and Y_{MeOH} can be obtained are about 97 and 91%, respectively, without violating the constraints on the

Table 6
Description of the multi-objective optimization problems solved in Case 2 together constraints, bounds of decision variables, and fixed parameters

Case	Objective	Constraint	Decision variable	Fixed variable
2	Max Y_{HOAc}, Max Y_{MeOH}	$X_{MeOAC} \geq 90\%$, $P_{HOAc} \geq 80\%$, $P_{MeOH} \geq 80\%$	$10 \leq t_s \leq 30$ min, $1.0 \leq \gamma \leq 3.0$, $0.1 \leq \beta \leq 0.9$, $1 \leq s \leq 3$, $1 \leq q$, $r \leq 2$	Same as Case 1 except $L = 30$ cm
2a			Same as Case 2 except χ (see Table 5)	Same as Case 2

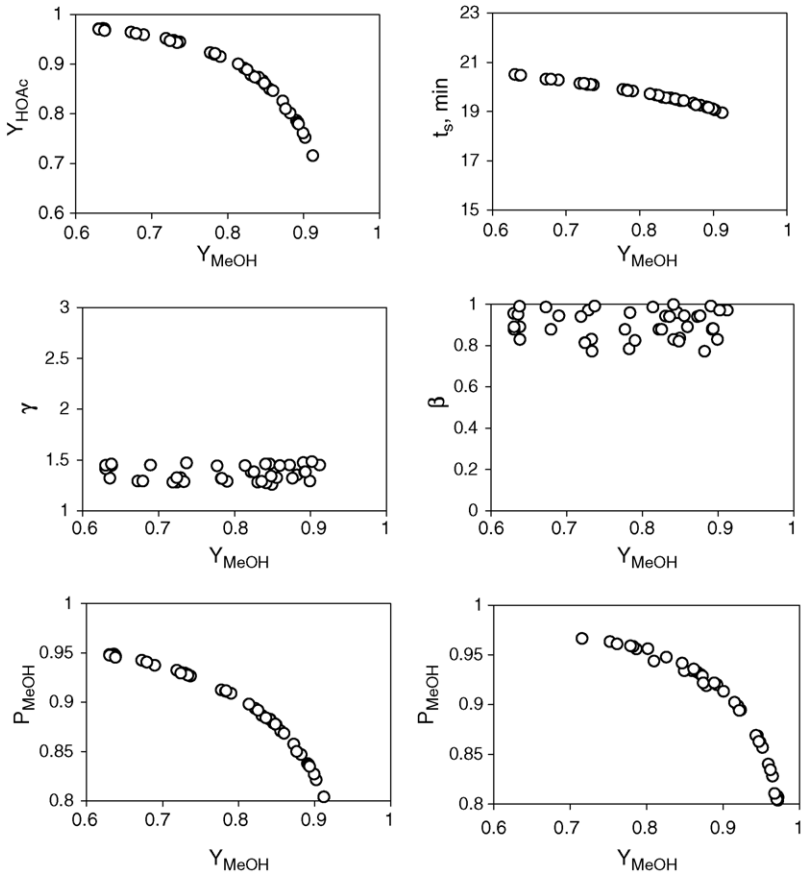

Fig. 12. Pareto optimal solutions and corresponding decision variables for the Case 2 optimization problem.

purity of both streams. The figure also shows that switching time is the key parameter in deciding the Pareto optimal solutions, and it decreases when Y_{MeOH} increases. The reduction of switching time increases the solid phase pseudo-velocity, and therefore, all components travel at a much faster rate with the solid phase, less methanol will breakthrough from section P, leading to higher Y_{MeOH}. Similarly, when switching time increases, all components will travel at a faster rate with the fluid phase, less amount of acetic acid will breakthrough from extract port increasing conversion and resulting in higher Y_{HOAc}. This can be clearly illustrated by comparing the concentration profiles at different switching time, as shown in Fig. 13. It was observed from Fig. 12 that raffinate flow rate and eluent flow rate are insensitive in determining the Pareto solutions. The performance of 7-column SMBR with respect of maximization of Y_{HOAc} and Y_{MeOH} was also

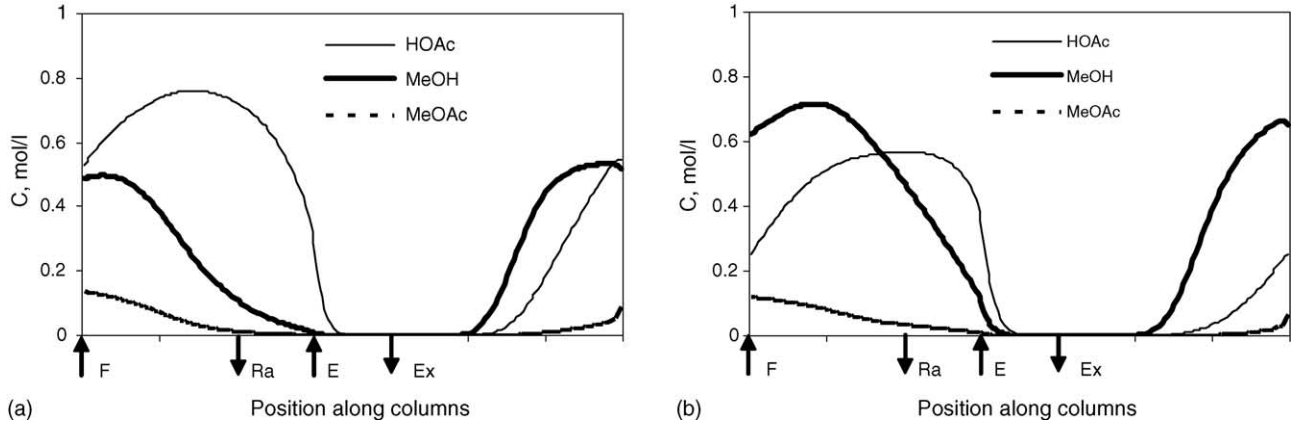

Fig. 13. Concentration profiles for MeOAc–HOAc–MeOH at the end of 100 switching for Case 2 optimization at two different t_s value. (a) t_s = 18 min and (b) t_s = 120 min.

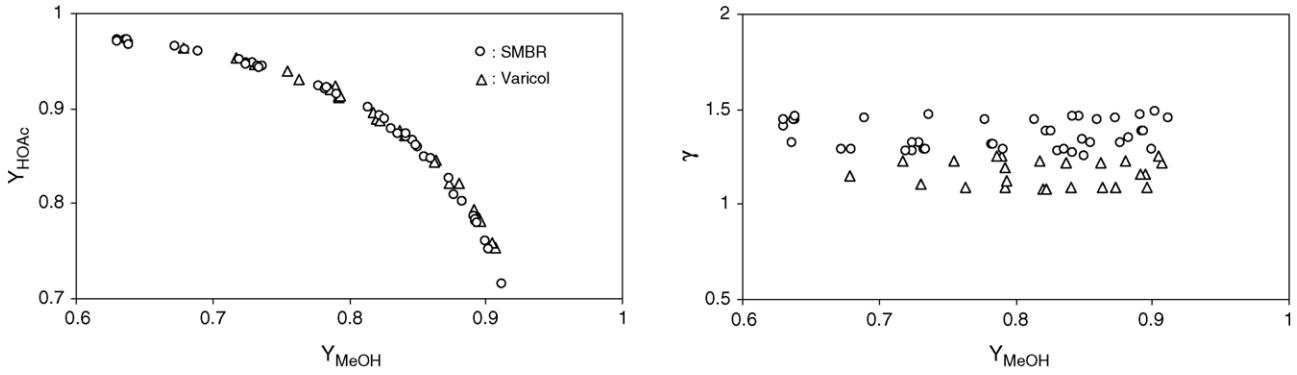

Fig. 14. Comparison of Pareto optimal solutions between a 7-column SMB and Varicol system (Case 2a).

compared with Varicol. Fig. 14 shows that there is no significant improvement in the Varicol system. However, the eluent consumption in Varicol is less than that for an equivalent SMBR, which is also shown in the figure.

4. Conclusion

Simulated Moving Bed (SMB) systems are used in industry for separations that are either impossible or difficult using traditional separation techniques. By virtue of its superior separating power, SMB has become one of the most popular techniques finding its application in petrochemical and sugar industries, and of late, there has been a drastically increased interest in SMB in pharmaceutical industry for enantio-separations. SMB systems can also be integrated to include reactions, which can provide economic benefit for equilibrium limited reversible reactions. In situ separation of the products facilitates the reversible reaction to completion beyond thermodynamic equilibrium and at the same time obtaining products of high purity. Recently, a new concept of non-synchronous switching instead of the synchronous one used in the traditional SMB technology is developed. The more flexible modified process (Varicol) was found to perform better than the rigid SMB system. However, the successful operation and implementation of separative and reactive SMB (as well as Varicol) processes on industrial scales will necessitate one to determine the optimal design parameters and operating conditions based on multiple objectives.

In this article, a comprehensive multi-objective optimization study of SMBR and Varicol systems for the hydrolysis of methyl acetate is reported. The non-dominated sorting genetic algorithm (NSGA) was used in obtaining Pareto optimal solutions. The multi-objective optimization problems were formulated aiming at simultaneous maximization of (a) and (b) yield of both the raffinate and the extract streams. The effects of column length, raffinate flow rate, eluent flow rate and distributed feed flow rate on the Pareto optimal solutions were investigated. The applicability of Varicol to reaction systems and the effect of number of sub-intervals on the performance of Varicol were also studied. It was observed that reactive Varicol performs better than SMBR due to its increased flexibility in column distribution. It is to be emphasized that there is no end of the variety of multi-objective optimization problems, which could be formulated and studied, and we have presented here, only a few simple examples, to illustrate the new optimization strategy and interpretation of results.

References

[1] Y. Fuchigami, Hydrolysis of methyl acetate in distillation column packed with reactive packing of ion exchange resin, J. Chem. Eng. Jpn. 23 (3) (1990) 354.
[2] S. Han, Y. Jin, Z. Yu, Application of a fluidized reaction-distillation column for hydrolysis of methyl acetate, Chem. Eng. J. 66 (1997) 227.
[3] K. Hashimoto, S. Adachi, H. Noujima, Y. Ueda, A new process combining adsorption and enzyme reaction for producing higher fructose syrup, Biotechnol. Bioeng. 25 (1983) 2371.
[4] A. Ray, A. Tonkovich, R.W. Carr, R. Aris, The simulated countercurrent moving bed chromatographic reactor: a novel reactor- separator, Chem. Eng. Sci. 45 (1990) 2431.
[5] A.K. Ray, R.W. Carr, R. Aris, The simulated countercurrent moving-bed chromatographic reactor—a novel reactor separator, Chem. Eng. Sci. 49 (1994) 469.
[6] A.K. Ray, R.W. Carr, Experimental study of a laboratory scale simulated countercurrent moving bed chromatographic reactor, Chem. Eng. Sci. 50 (1995) 2195.
[7] A.K. Ray, R.W. Carr, Numerical simulation of a simulated countercurrent moving bed chromatographic reactor, Chem. Eng. Sci. 50 (1995) 3033.
[8] M. Mazzotti, A. Kruglov, B. Neri, D. Gelosa, M.A. Morbidelli, Continuous chromatographic reactor: SMBR, Chem. Eng. Sci. 51 (1996) 1827.
[9] M. Kawase, T.B. Suzuki, K. Inoue, K. Yoshimoto, K. Hashimoto, Increased esterification conversion by application of the simulated moving-bed reactor, Chem. Eng. Sci. 51 (1996) 2971.
[10] M. Meurer, U. Altenhoner, J. Strube, A. Untiedt, H. Schmidt-Traub, Dynamic simulation of a simulated-moving-bed chromatographic reactor for the inversion of sucrose, Starch/Starke 48 (1996) 452.
[11] F. Lode, M. Houmard, C. Migliorini, M. Mazzotti, M. Morbidelli, Continuous reactive chromatography, Chem. Eng. Sci. 56 (2001) 269.
[12] Z. Zhang, K. Hidajat, K.A.K. Ray, Application of simulated countercurrent moving bed chromatographic reactor for MTBE synthesis, Ind. Eng. Chem. Res. 40 (2001) 5305.

[13] D.C.S. Azevedo, A.E. Rodrigues, Design methodology and operation of a simulated moving bed reactor for the inversion of sucrose and glucose-fructose separation, Chem. Eng. J. 82 (2001) 95.
[14] O. Ludemann-Hombourger, R.M. Nicoud, M. Bailly, The "VARICOL" process: a new multicolumn continuous chromatographic process, Sep. Sci. Technol. 35 (12) (2000) 1829.
[15] C. Migliorini, M. Fillinger, M. Mazzotti, M. Morbidelli, Analysis of simulated moving bed reactors, Chem. Eng. Sci. 54 (1999) 2475.
[16] G. Dunnebier, J. Fricke, K.K. Klatt, Optimal design and operation of simulated moving bed chromatographic reactors, Ind. Eng. Chem. Res. 39 (2000) 2290.
[17] D.C.S. Azevedo, A.E. Rodrigues, Design methodology and operation of a simulated moving bed reactor for the inversion of sucrose and glucose-fructose separation, Chem. Eng. Sci. 82 (2001) 95.
[18] V. Bhaskar, S.K. Gupta, A.K. Ray, Applications of multiobjective optimization in chemical engineering, Chem. Rev. 16 (2000) 1.
[19] K. Deb, Multi-Objective Optimization using Evolutionary Algorithms, Wiley, Chichester, UK, 2001.
[20] A.D. Nandasana, A.K. Ray, S.K. Gupta, Applications of non-dominated sorting genetic algorithm in chemical reaction engineering, Int. J. Chem. Reactor Eng. 1 (R2) (2003) 1.
[21] W. Yu, K. Hidajat, A.K. Ray, Modeling, simulation and experimental study of simulated moving bed reactor for the synthesis of methyl acetate ester, Ind. Eng. Chem. Res. 42 (2003) 6743.
[22] W. Yu, K. Hidajat, A.K. Ray, Determination of kinetic and adsorption parameters for methyl acetate esterification and hydrolysis reaction catalyzed by Amberlyst 15, Appl. Cat. B: General 260 (2) (2004) 191.
[23] Y. Zang, P.C. Wankat, SMB operation strategy-partial feed, Ind. Eng. Chem. Res. 41 (2002) 2504.
[24] Y. Zang, P.C. Wankat, Three-zonr simulated moving bed with partial feed and selective withdrawal, Ind. Eng. Chem. Res. 41 (2002) 5283.
[25] Z. Zhang, M. Mazzotti, M. Morbidelli, PowerFeed operation of simulated moving bed units: changing flow-rates during the switching interval, J. Chromatogr. A 1006 (2003) 87.
[26] Z. Zhang, M. Mazzotti, M. Morbidelli, Experimental assessment of PowerFeed chromatography, AIChE J. 50 (2004) 625.
[27] Z. Zhang, M. Mazzotti, M. Morbidelli, Continuous chromatographic processes with a small number of columns: comparison of simulated moving bed with Varicol, PowerFeed, and ModiCon, Korean J. Chem. Eng. 21 (2004) 454.
[28] Z. Zhang, K. Hidajat, A.K. Ray, M. Morbidelli, Multiobjective optimization of SMB and Varicol process for chiral separation, AIChE J. 48 (2002) 2800.